An NMR Self-Diffusion Investigation of Aggregation Phenomena in Solutions of Ethyl(hydroxyethyl)cellulose

Magnus Nydén* and Olle Söderman

Department of Physical Chemistry 1, Center for Chemistry and Chemical Engineering, Lund University, P.O. Box 124, S-221 00 Sweden

Received October 7, 1997; Revised Manuscript Received February 10, 1998

ABSTRACT: Water solutions of ethyl(hydroxyethyl)cellulose have been investigated with the PFG NMR technique and by means of ^{1}H NMR relaxation measurements. The echo decays in PFG experiments have been recorded for EHEC with concentrations ranging from the dilute ($c < c^*$) to the semidilute ($c > c^*$). In addition, the temperature dependence of the echo decay was investigated. It is shown that the echo decays deviate substantially from Gaussian diffusion behavior. We discuss this in terms of polydispersity, aggregation, and scaling effects. It is argued that the observed deviations are too large to be caused by polydispersity effects alone. We base this conclusion on the observation that the molar mass scaling of the polymer diffusion coefficient goes roughly as M^{-4}. We focus on using a log-normal distribution of diffusion coefficients in the evaluation procedure of the PFG data. It is found that by comparing the diffusion coefficients extracted from this type of procedure with "D_{mean}" as extracted from a "stretched exponential" approach, there is a difference in the evaluated diffusion constant by up to 1 order of magnitude. The difference depends on the degree of deviation from linear behavior in the echo decay when represented in a logarithmic plot vs the relevant experimental parameter.

Introduction

A polymer with a *hydrophobic* backbone, for example, polyethylene, is only slightly soluble in water. However, it can be made water soluble by covalently attaching water soluble chains to the backbone. An example of a different kind of polymer is ethyl(hydroxyethyl)cellulose, henceforth referred to as EHEC. The introduction of covalently bound ethylene oxide and ethyl groups randomly attached to the cellulose backbone makes EHEC water soluble up to high concentrations. The reason EHEC is soluble in water is most likely due to the breaking/destabilization of the crystal structure on account of the introduction of the side chains. The backbone of EHEC is made up of β-D-glucose, linked by β-1,4-glucoside bonds. The structures of EHEC and EHEC100 (the hydrophobic modified version of EHEC) are shown in Figure 1. EHEC has found extensive use in a wide range of applications.

The interactions of various types of EHEC (with different kinds of modifications) with surfactants[1−7,9−13] and other types of polymers[10] have been thoroughly investigated in previous works. Thuresson has extensively compared the hydrophobically modified EHEC, termed EHEC100 in this work, with the hydrophobically unmodified polymer with regard to the interactions with surfactants and other cosolutes.[11] In contrast, little attention has been paid to the behavior of the pure EHEC polymer in solution. This work is focused on the behavior of the pure EHEC polymer in solution.

A number of previous papers[14−18] describe the influence of size polydispersity on the PFG NMR experiment performed in polymer systems. It is generally observed that when there is a large polymer polydispersity, the echo intensities show a nonlinear decay, when plotted on a log scale vs the parameter $k = (\gamma g \delta)^2(\Delta - \delta/3)$ (from here on referred to as a Stejskal−Tanner plot), where γ is the proton magnetogyric constant, δ is the length of the gradient pulse, g is the gradient strength, and Δ is the time separation between the gradient pulses. However, the degree of deviation from linearity is in most cases less than what would be predicted for a polydisperse polymer solution, in which every polymer diffuses independently of the rest of the polymers. From a fit to the experimental data it is in principle possible to extract information of the molar mass scaling exponent of the diffusion coefficient, the mean molar mass, and the size distribution (assuming an appropriate distribution function).

Callaghan and Pinder[14] measured the diffusion coefficient in mixtures of dextran and water. In their paper, the polydispersity was treated by assuming that the echo decay could be described by a mass average of the diffusion coefficient. One of their conclusions was that there is an averaging process between diffusion constants of slow and fast diffusing molecules. This conclusion was based on the observation that the curvatures in the echo decay plots were less than expected from the known distribution of molar masses. They discussed different such averaging processes, one being the interaction acting through the collisions of the polymers and also the hydrodynamic interactions acting through the solvent as depicted by the Kirkwood-Riesemann theory. The effect of averaging was also seen when mixing two polymers with different molar masses and narrow size distributions.

Fleischer[16] also investigated the effect of polydispersity in PFG NMR data, using polystyrene in toluene solutions. He found that, for large polydispersities, the echo decays were nonlinear in a Stejskal−Tanner plot and proceeded to evaluate the echo decay data by assuming a log-normal distribution of molar masses and a diffusion coefficient molar mass dependence according to $D = KM^{-\alpha}$ and then argued that the exponent α should range from 0.5 (for a Θ solvent) at high dilution, to 2 for concentrations well above the overlap concentration (c^*). The results from Fleischer's work showed

* Corresponding author. Tel.: +46 46 22 20 112. Fax: +46 46 22 20 112. E-mail: Magnus.Nyden@fkem1.lu.se.

S0024-9297(97)01472-1 CCC: $15.00
Published on Web 07/03/1998

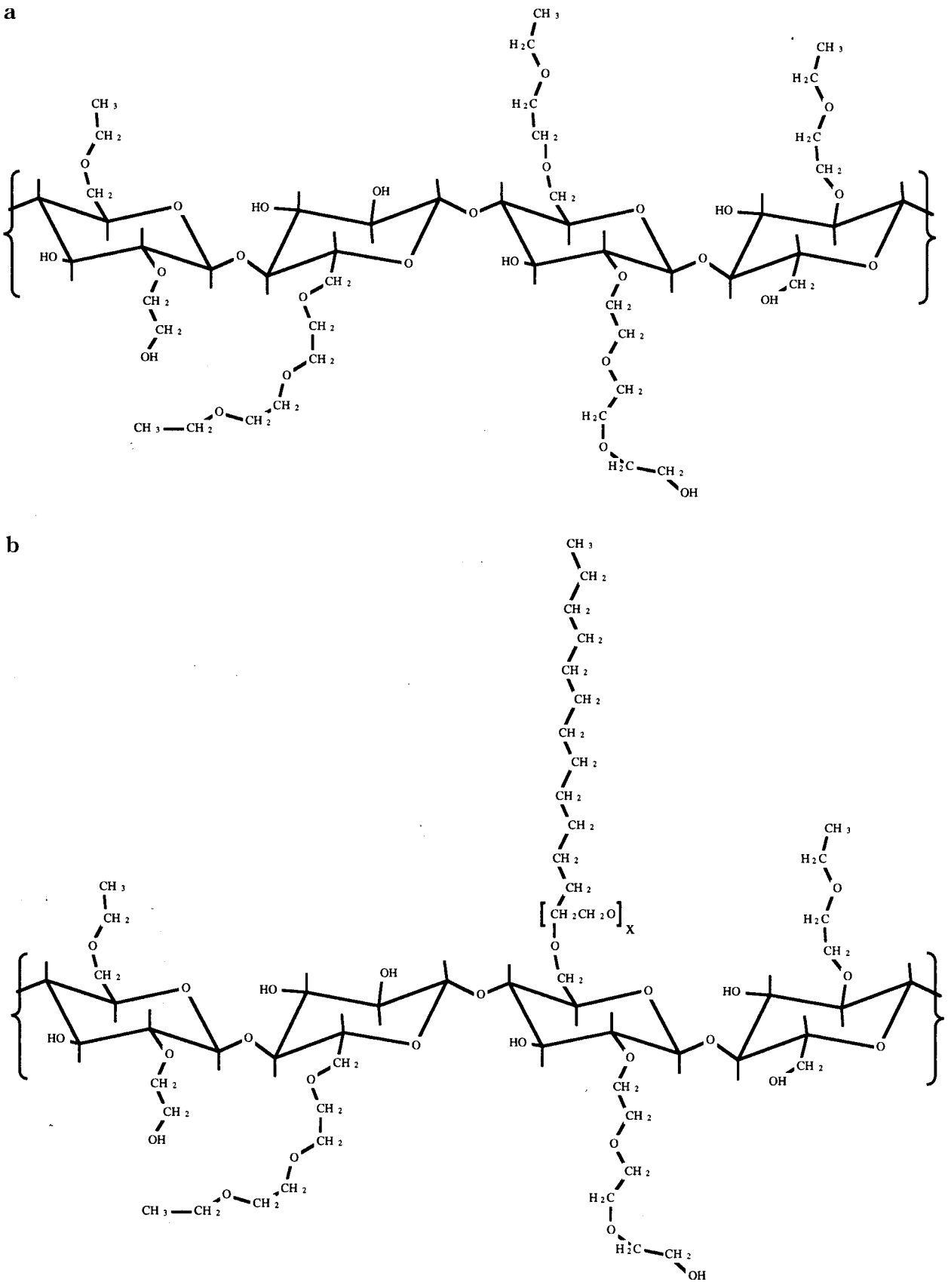

Figure 1. Structure of EHEC (a) and EHEC100 (b). Note that this is not by any means an exact structure, which is most certainly very complex with different degrees of substitutions of the various side chains along the backbone.

that the theory could describe the experimental data. However, he also concluded that there is some kind of mechanism acting to average the diffusion coefficients for polymers differing in size.

In this work we have attempted to compare different types of evaluation approaches concerning the interpretation of the echo decay curvature in PFG NMR data from polymer solutions. We choose to measure the echo

decay down to the noise level when possible. We will report results from PFG NMR self-diffusion measurements of polydisperse EHEC polymers in water solutions where the concentration is ranging from the dilute to the semidilute region. In addition, we investigate the polymer diffusion behavior as function of temperature. The echo decays have been followed over an extended range of gradient strengths. We argue that there is a curvature in the echo decay plot that is *larger* than the curvature that would result from the distribution of molar masses in the EHEC samples studied. Different reasons for the presence of these curvatures will be discussed.

Experimental Section

Materials. Both EHEC and EHEC100 were supplied by Akzo Nobel Surface Chemistry AB, Stenungsund, Sweden. The average molar mass for both polymers is around 200 000 g/mol, with a typical polydispersity index of 2−3.[4] The EHEC degree of substitution was 0.6−0.7 for ethyl and 1.8 for the hydroxyethyl groups. These numbers correspond to the average number of substitution per glucose unit of the backbone. EHEC100 was synthesized according to the same method as EHEC, with the same degree of substitution of ethyl and hydroxyethyl groups. The hydrophobic modification of EHEC100 consists of (on average) one hydrophobic group per 100 glucose units. To remove salt and other material present in the synthesis of EHEC100, it was purified in acetone to remove nonreacted hydrophobic molecules. Then the polymer powder was dissolved in water and molecules that were not water soluble were removed by centrifugation. As a last step, salt was removed by dialyzing against Millipore water using a Filtron Ultraset setup. The dialyzation was stopped once the conductivity of the solution was below 2 μS/m. The procedure for the purifying of EHEC was the same as for EHEC100 except for the extraction in acetone, which was not performed for EHEC. All concentrations quoted in this work will be given in weight percent.

Methods. The NMR spectrometer used for all diffusion and relaxation experiments was a Bruker DMX 200. Pulse sequences used for the diffusion measurements were the stimulated echo and the Hahn echo. For the stimulated echo, a phase cycling of 16 steps was used to isolate the desired echo. The measurements can be performed with varying gradient length (δ) or gradient strength (g). In this work we have mainly used the latter method since we have detected no mismatch problem or any nonlinearity in the amplifier. As a general rule we used the Hahn echo sequence for measurements when the "T_2" relaxation showed a single-exponential decay and the stimulated echo for samples with smaller values of T_2 and/or when the relaxation curve showed a deviation from the single-exponential decay. The inversion−recovery curves were well described with a single T_1 for all the concentrations investigated and consequently most measurements were performed with the stimulated echo sequence with the time between the first two 90° pulses as short as possible (typically 2−3 ms).

The probe used for measurements when the diffusion coefficients were not too slow was a Bruker gradient probe with the capacity to deliver gradient pulses of maximum 9 T/m at a current of 40 A. For measurements where the diffusion coefficients were very slow and/or the relaxation was fast, a probe with a home-built quadrupolar coil capable of giving 100 T/m working at 40 A was used. The measurements performed at high temperatures were checked for temperature gradient induced flow by measuring the water diffusion. Any flow occurring from temperature gradients would give rise to a time dependent water diffusion coefficient. No such dependence was detected at the temperatures used. The relaxation measurements were performed by using the CPMG sequence. All data evaluation was performed by a Levenberg−Marquart fitting procedure, using the Matlab package on Machintosh computers. If not stated otherwise, all measurements were performed at 19 °C.

Theoretical Considerations

The NMR self-diffusion technique enables the measurement of the true *self-diffusion* of molecules and thus it is a very powerful technique for the elucidation of various dynamical aspects of many chemical systems. The theoretical treatment of the dynamics in the case of unrestricted diffusion of a single species with fast exchange between different diffusion sites when compared to the experimental diffusion time is straightforward. However, when the diffusion is hindered or in any way deviates from free diffusion, the situation can be more complex.

In this paper we address the problem of overlapping NMR spin-echo signals arising from molecules with different molar masses. A general complication is the fact that different diffusion mechanisms can affect the echo decay in similar ways and hence the elucidation of the true diffusion mechanism can be difficult.

In general, the echo decay is a Fourier transformation of the propagator, $P_s(\vec{r}|\vec{r}',\Delta)$ according to the following expression[19]

$$E(\vec{q},\Delta) = \int \rho(\vec{r}) \int P_s(\vec{r}|\vec{r}',\Delta) \exp[i2\pi\vec{q}\bullet(\vec{r}' - \vec{r})]\, d\vec{r}'\, d\vec{r} \quad (1)$$

where $\vec{q}$ is the "wave vector" given by $(1/2\pi)(\gamma\delta\vec{g})$, $\rho(\vec{r})$ is the spin density, and $P_s(\vec{r}|\vec{r}',\Delta)$ is the probability for a molecule to move from $\vec{r}$ to $\vec{r}'$ during time Δ. Equation 1 can be simplified to give

$$E(\vec{q},\Delta) = \int P(\vec{R},\Delta) \exp(i2\pi\vec{q}\bullet\vec{R})\, d\vec{R} \quad (2)$$

were $P(\vec{R},\Delta)$ is the average propagator, which is the probability that a molecule is displaced a distance $\vec{R} = \vec{r}' - \vec{r}$ during the time Δ, independent of starting position. In the case of unrestricted diffusion, the propagator is Gaussian, with the diffusion coefficient given by the width of the Gaussian. If the measurements are performed under the narrow pulse approximation and the propagator is Gaussian, eq 2 gives the mean square displacement according to

$$E(\vec{q},\Delta) = \exp(-2\pi^2 q^2 \langle z^2 \rangle) \quad (3)$$

If the polymers are polydisperse in size, the echo decay is given by[16]

$$E(\vec{q},\Delta) = \frac{\int_0^\infty A(M) \exp(-4\pi^2 q^2 D(M)\Delta)\, dM}{\int_0^\infty A(M)\, dM} \quad (4)$$

where $A(M)$ is a distribution function for the molar masses. $D(M)$ is the dependence of the diffusion coefficient on the molar mass.

The log-normal distribution is an often used description for the molar mass distribution in polymer systems:[16]

$$A(M) = \frac{1}{M\left(2\pi \ln\left(\frac{\bar{M}_w}{\bar{M}_n}\right)\right)^{1/2}} \exp\left(-\frac{\left(\ln(M) - \ln\left(\sqrt{\frac{\bar{M}_w}{\bar{M}_n}}\right)\right)^2}{2 \ln\left(\frac{\bar{M}_w}{\bar{M}_n}\right)}\right) \quad (5)$$

where $\bar{M}_w$ is the weight average molar mass and $\bar{M}_n$ is the number average molar mass. The dependence of the diffusion coefficient on the molar mass can be written as a scaling relation according to

$$D = KM^{-\alpha} \quad (6)$$

where K is a constant and α is a scaling parameter. However, experimentally, it is found that this relation is seldom valid over a large range of molar masses.[20]

Another type of scaling relation is provided by Phillies[20−25] and is of the form

$$D = D_0 \exp(-aM^{\nu}) \quad (7)$$

where D_0 is the diffusion coefficient at infinite dilution and a and ν are scaling parameters. In conclusion, the echo attenuations can be described by eqs 4 and 6

$$E(\vec{q},\Delta) = \frac{\int_0^\infty A(M) \exp(-4\pi^2 q^2 K M^{-\alpha}\Delta)\, dM}{\int_0^\infty A(M)\, dM} \quad (8)$$

or eqs 4 and 7, depending on the way one wishes to describe the data,

$$E(\vec{q},\Delta) = \frac{\int_0^\infty A(M) \exp(-4\pi^2 q^2 D_0 \exp(-aM^{\nu})\Delta)\, dM}{\int_0^\infty A(M)\, dM} \quad (9)$$

Since eqs 8 and 9 cannot be solved analytically, they have to be fitted to the experimental data using numerical procedures.

Another approach is to fit a stretched exponent of the form

$$E(\vec{q},\Delta) = \exp[(-4\pi^2 q^2 D_{app}\Delta)^{\beta}] \quad (10)$$

to the data. Here D_{app} is an apparent diffusion coefficient and β is the "streching exponent". This approach has been used in a number of previous works.[8,12,26−28] One obtains the inverse mean diffusion coefficient[29] through the relation

$$\left\langle \frac{1}{D} \right\rangle = \frac{\frac{1}{\beta}\Gamma\left(\frac{1}{\beta}\right)}{D_{app}} \quad (11)$$

where Γ is the gamma function. As first pointed out by Callaghan, a source of complication is the fact that $\langle 1/D\rangle^{-1} \neq \langle D\rangle$. This means that the calculated diffusion coefficient will be strongly weighted by slowly diffusing species as the curvature in the echo decay increases (β decreases from unity).

In the thesis by Lindell,[4] the molar mass distribution for EHEC has been measured by size exclusion chromatography and the result is shown in Figure 2. The

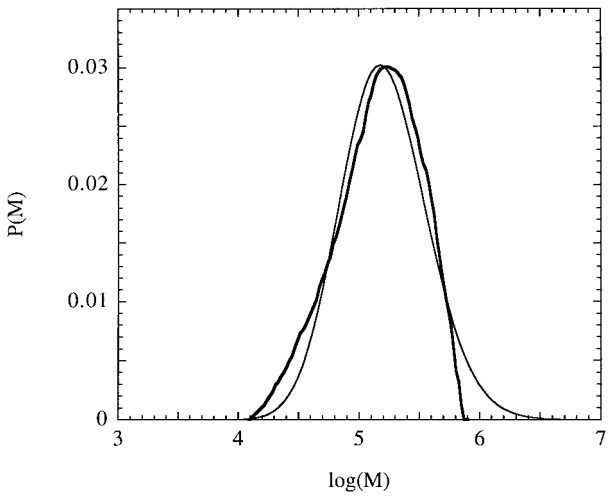

Figure 2. Weight average of the distribution of molar masses for EHEC. The data are reproduced from the thesis by Lindell[4] (thick line). Shown also is the fit of the log-normal distribution of molar masses (thin line).

data presented in Figure 2 are measured for a different batch of EHEC than the one used in this work. However, data from three different batches of EHEC were presented and it was noted that even though they differed in both in molecular weight and cloud point, their size distributions were similar.[4] The data (thick line) show some resemblance to the fit of a log-normal distribution of molar masses (thin line). However, there are some deviations from the log-normal distribution. With this in mind we fitted the distribution given by Lindell to a polynomial so that the echo decay would depend on the molar mass as follows

$$E(\vec{q},\Delta) = \{\int_{M1}^{M2}(P_1M + P_2M^2 + P_3M^3 + P_4M^4 + P_5M^5) \exp(-4\pi^2 q^2 D(M)\Delta]\, dM\}/\{\int_{M1}^{M2}(P_1M + P_2M^2 + P_3M^3 + P_4M^4 + P_5M^5)\, dM\} \quad (12)$$

were P_i are expansion coefficients.

Finally, we have investigated whether the NMR PFG data can be fitted to a log-normal distribution of diffusion coefficients of the form

$$E(\vec{q},\Delta) = \int_0^\infty \frac{1}{D\sigma\sqrt{2\pi}} \exp\left[-\left(\frac{\ln(D) - \ln(D_m)}{\sqrt{2\sigma}}\right)^2\right] \times \exp(-4\pi^2 q^2 D\Delta)\, dD \quad (13)$$

were D_m is the mass-weighted median diffusion coefficient and σ gives the width of the distribution. For reasons that will be explained later in the text, we will modify eq 13 to include the possibility of a log-normal distribution of diffusion coefficients plus a single diffusing component. This is expressed in eq 14

$$E(\vec{q},\Delta) = f \exp(-4\pi^2 q^2 D_s\Delta) + (1 - f)\int_0^\infty \frac{1}{D\sigma\sqrt{2\pi}} \times \exp\left[-\left(\frac{\ln(D) - \ln(D_m)}{\sqrt{2\sigma}}\right)^2\right] \exp(-4\pi^2 q^2 D\Delta)\, dD \quad (14)$$

where f is the fraction of polymers that diffuses with a single (slow) diffusion coefficient D_s. The other parameters have their usual meaning.

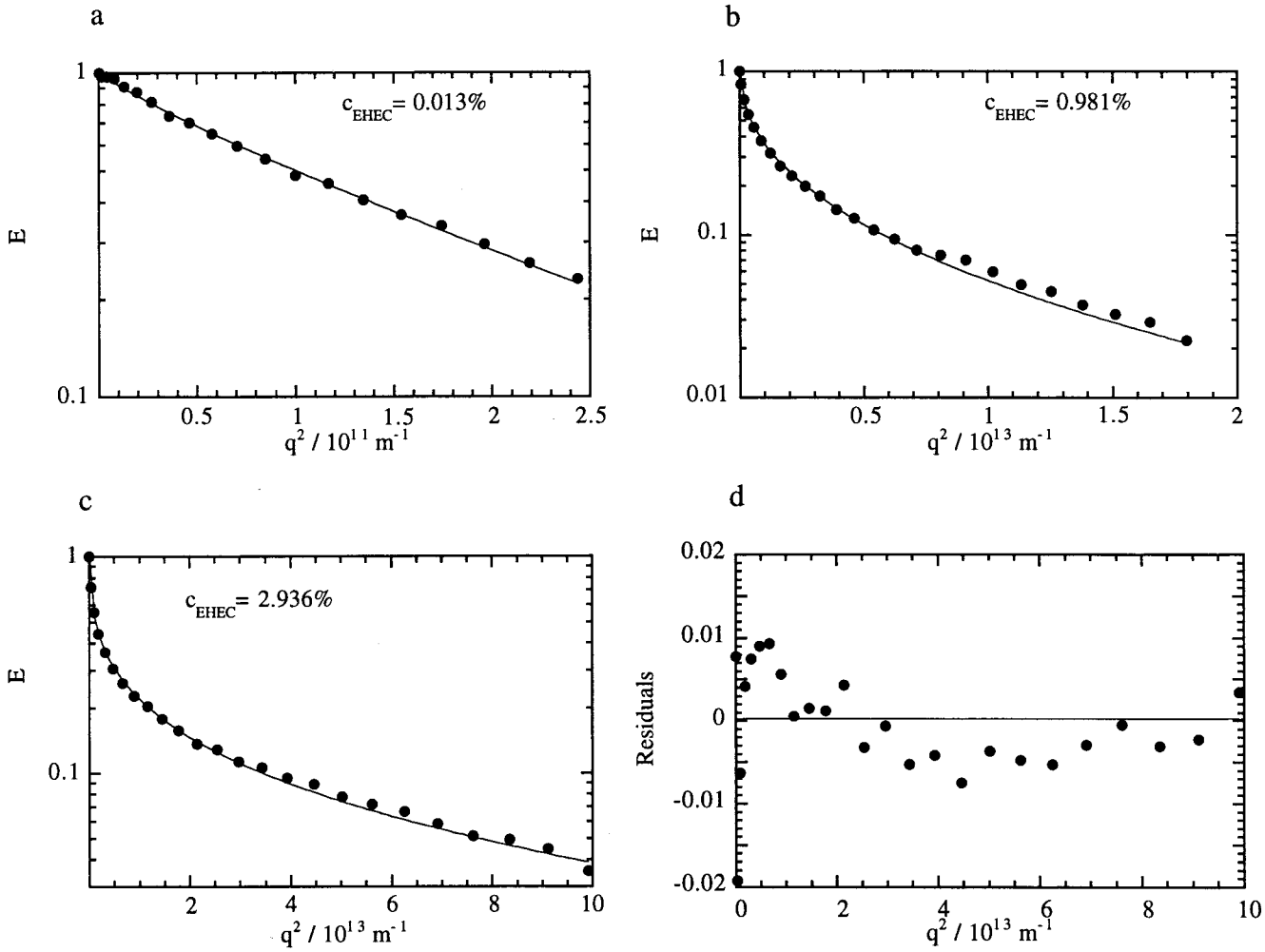

Figure 3. Echo decays for three different concentrations of EHEC: (a) 0.013%; (b) 0.981%; (c) 2.936% EHEC. The full lines are the results from fits of eq 10 to the data. (d) Residuals from the fit of eq 10 to the 2.936% data set. It is clear that the residuals are not random.

Considerations Concerning the Evaluation Method. In this section we will describe the various approaches used in treating the PFG NMR data (as described by eqs 8−10, and 12−14). To do this, we present the results of fitting these eqs to the EHEC data.

1a. Stretched Exponential. In Figure 3a−c we show the fits of eq 10 to three data sets, corresponding to 0.013%, 0.981%, and 2.93% EHEC. It is clearly seen that the stretched exponential describes the data reasonably well over the concentration range. (We note that a convenient way to investigate the goodness of the fit of a stretched exponential to the data, is to plot log(E) vs $q^{2\beta}$.) Despite the problems with the stretched exponential approach (see above), we have chosen to present the results from the stretched exponential analysis, bearing in mind that the "D_{mean}" values are strongly influenced by slowly diffusing species.

1b. Log-Normal Distribution of Molar Masses. For the samples with low concentrations of polymers, the use of eq 4 (with $\alpha = 0.5$) gives a molar mass distribution close to the one measured in the work by Lindell.[4] However, for higher concentrations the obtained distribution becomes too wide. [Experiments performed on a probe polymer diffusing in an EHEC matrix indicate that the molar mass scaling exponent, α, is approximately 1 for the probe polymer when the EHEC concentration is 1 wt %. The probe molecule used in those experiments is poly(ethylene oxide), which was added in trace amounts (to be published). If we use this number for α, we obtain $\bar{M}_w/\bar{M}_n = 4$ for the 0.981% sample, which indicates a very large spread in molar mass.] We also note that the use of eq 9 works equally as well as eq 8 in describing the data. However, the scaling exponent in eq 7 takes on large values in order to account for the curvature in the echo decay. *Consequently, it would appear that the obtained molar mass distributions are too wide to reflect the intrinsic polydispersity of the polymer sample, when the concentration increases.*

At first this might seem natural since EHEC has self-aggregating properties (see further discussion below). However, it is not clear why the lifetime of the aggregates is longer than the time scale of the experiment, which is around 1 s.

1c. Known Distribution of Molar Masses. We have also examined the fit of eq 12 (data not shown) to two data sets for EHEC: 0.013% and 0.981%. We conclude that eq 12 fits the data very well. However, the value obtained for α ($\alpha = 4$) is yet another indication that the observed curvatures in the echo decays are probably *not an effect arising from polymer polydispersity in size alone.*

1d. Log-Normal Distribution of Diffusion Coefficients. The results of using eq 13 for three different concentrations of EHEC are shown in Figure 4. The

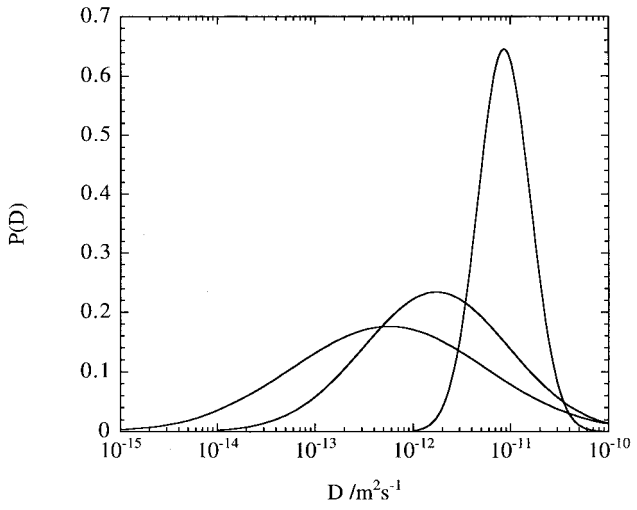

Figure 4. Distribution of diffusion coefficients according to the results of eq 13 for three concentrations of EHEC: 0.013%, 0.981%, and 2.936%. The figure is an attempt to visualize that as the curvature in the echo decay data increases, this is accompanied by an increase in the distribution width of the diffusion coefficients. Note that the curves are not normalized.

concentrations are 0.013%, 0.981%, and 2.93% EHEC. Eq 13 fits the data well over the concentration region (data not shown).

Choice of Evaluation Procedure of PFG Data. We are now at a stage where we may decide which evaluation routine to use of the four described above. It is clear that eqs 8 and 9 describe the data well. However, we note that the scaling exponents (using both eq 6 and 7) are large and we conclude that the polydispersity in the molar masses alone cannot be the cause of the observed curvatures in the echo decays. As mentioned above, eq 10 has some disadvantages, the main problem being the fact that D_{mean} is not the true mean diffusion coefficient but rather is weighted by slowly diffusing components. Equation 12 gave good fits to the data. However, the results indicated a strong scaling of the diffusion coefficient with the molar mass.

At this stage it should be mentioned that one additional way of evaluating the echo decay is by using a Contin analysis,[30] where no assumption about the actual shape of the distribution of diffusion coefficients is made. However, the method relies on high-quality data. This is very time consuming to obtain when the polymer concentration is low.

For reasons mentioned above, we have chosen to use eqs 13 and 14 in the evaluation procedures from here on.

Results and Discussion

Introduction. The echo decays in EHEC solutions are generally curved when plotted in a Stejskal−Tanner plot. The curvature may be caused by several mechanisms. First of all, the size polydispersity of the polymer molecules may play a role. We note, however, that only polymers with a very high polydispersity index give rise to curved echo decays.[14,16]

Second, the aggregation of polymer molecules itself can give rise to an apparent polydispersity in the polymer size. With this in mind, we note that the substitution of OH groups for ethylene oxide is a process that most likely leads to a "blocky" structure of the polymer backbone, since the attachment of these groups is almost certainly not homogeneous along the backbone. As a consequence, a nonhomogeneous structure can be formed, as visualized in Figure 5. This situation implies that the polymer contains parts of the backbone that are substituted to a low degree and, consequently, these parts will have a tendency to form crystalline cellulose type structures, the presence of which may provide a mechanism for both inter- and intramolecular interactions.

Moreover, we note that ethyl and ethylene oxide groups are not present in a random fashion along the backbone. Preliminary results[52] indicate that the ethyl groups are found where the fraction of ethylene groups is low along the backbone and vice versa. In water, the ethyl groups would then give rise to hydrophobic interactions. This is another possible background of the associative properties observed for these polymers.

In this context it is interesting to consider the effects of addition of SDS to the hydrophobically modified polymer. Working with a polymer concentration of 1% EHEC100, Nyström et al.[54] found that at a certain SDS concentration, there was a maximum in the viscosity. The PFG data for a similar system[53] showed that when SDS was added to the solution, the curvature in the echo decays became more pronounced. As the SDS concentration was increased further, the curvature reached a maximum at the same SDS concentration where the viscosity maximum was observed. When the SDS concentration was further increased beyond the viscosity maximum, the number of micelles increased, thus decreasing the possibility for network formation. As a result, the viscosity decreased as did the curvature in the echo decay. Based on the discussion above, we will in the next section discuss in more detail the different effects that give rise to the observed curvatures in the echo decays.

Molar Mass Polydispersity and Aggregate Polydispersity. As pointed out by other authors,[14−16] there appears to exist an averaging process of diffusion coefficients for species of different size in solution. This has been observed in continuous distributions of molar masses in polymer solutions[14−16] and in solutions with a bimodal mixture of molecules differing in size and diffusion coefficients.[15] In particular, the results showed that for polymers with a distribution in molar masses, the echo decays were less curved than what would be expected from the known distribution and the "known" diffusion coefficient scaling of the molar mass. The results are by no means suprising, but the mechanism for the averaging process is still under debate.

Another possible mechanism for the observed echo decays is the micro/macro heterogeneities that can be found in any system close to a phase separation. These heterogeneities can extend over several different length scales. Since the polymers under study here phase separate (into two liquid solutions) as the temperature is increased (phase separation temperature for EHEC100 is 45 °C, and for EHEC 75, °C), this kind of mechanism is likely to be of importance. The criterion for this effect to influence the echo decay is that the lifetime of the clusters is sufficiently long as compared to the time scale of the measurement. If this is the only effect causing the curvature, it will be difficult to evaluate the data in a quantitative way, since the molar mass scaling exponent, α (assuming eq 6 is used in describing the molar mass scaling), then becomes a function of the molar mass. This is a consequence of the fact that the value of α is a measure of the mechanism for diffusion,

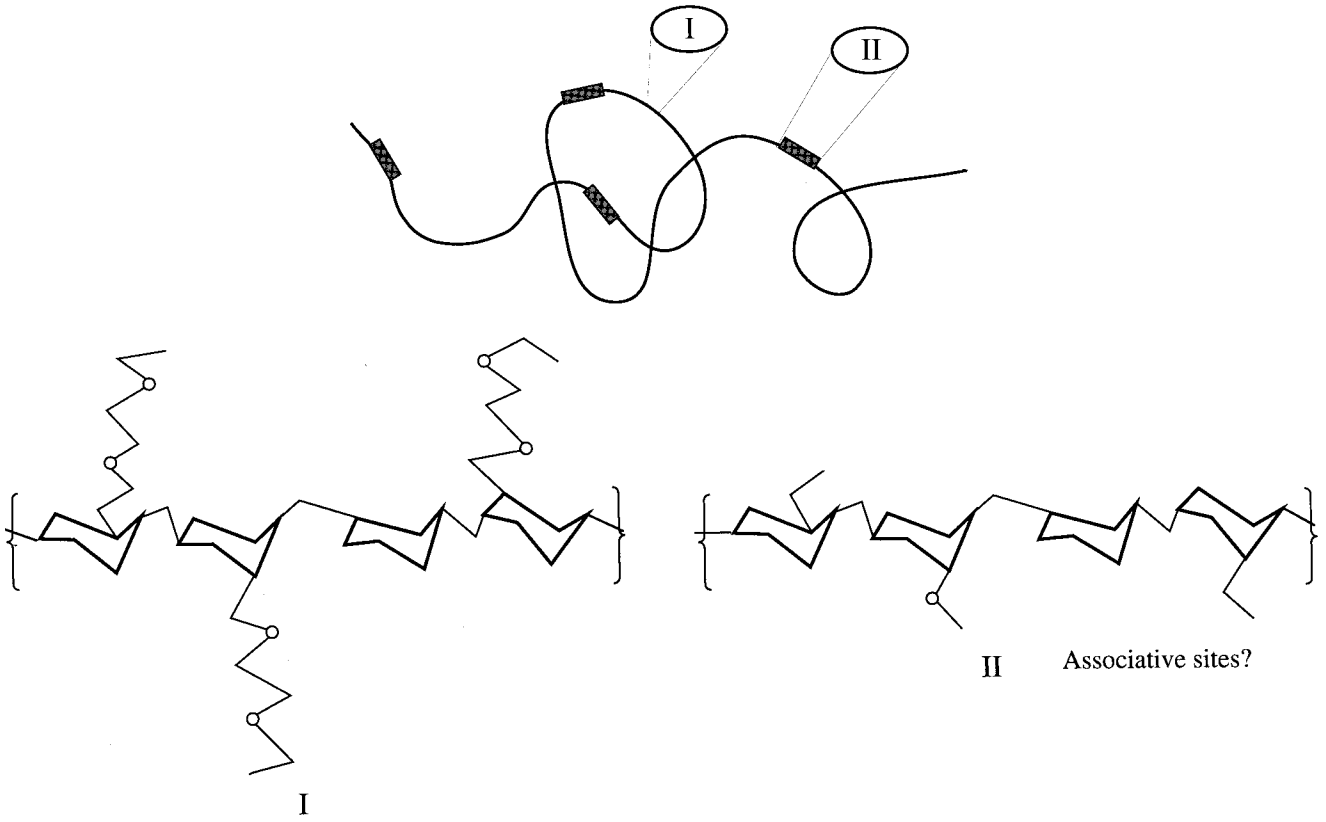

Figure 5. Schematic picture of the "blocky" structure of EHEC. The blockiness is due to the inhomogeneous distribution of the various side chains on the cellulose backbone. However, it is an open question what mechanism is responsible for the strong attraction acting between the polymers.

as can be seen in the concentration dependence of α. If the polymers differ extensively in size, it is conceivable that the diffusion mechanism for large clusters differs from that of small diffusing polymers even at one fixed concentration. In addition, the lifetime of the aggregates are unknown and as a consequence the theory development will be complicated.

Influence of Networks. We now turn to the nature of the microstructures formed by the aggregating polymer molecules. Since this study is made from the dilute to semidilute region, the system will pass through c^*, which is approximately 0.1% and at which concentration polymer molecules will start to overlap. A well-known theory for polymer diffusion for semidilute solutions and in the melt is based on the reptation model. This model is valid only for nonaggregating and monodisperse polymer systems and has been extensively investigated with several different experimental techniques, such as neutron scattering,[32] PFG NMR,[33,34] dynamic light scattering,[35] and fluorescence microscopy.[36−38] For EHEC the situation is quite different since the polymer is by no means monodisperse and also probably forms a physical network (not to be confused with the network formed above c^* for a nonaggregating polymer) on account of the polymer−polymer interactions discussed above. This means that when the physical network is formed, it is difficult to predict α, since the larger polymers will be more hindered than the small polymers, and hence, in the network the diffusion mechanism can differ for different size polymers. However, it seems likely that network formation will enhance the scaling exponent, partly due to the formation of heterogeneities.

An example of this behavior is seen in the work of Muthukumar and Baumgartner.[39−42] These authors simulated a situation in which molecules of different lengths were allowed to diffuse in a heterogeneous media. They found that α increased from 2 to 3, when heterogeneities were introduced in a system with strong topological constraints. One parameter that then becomes important is the polydispersity of the network pores. If part of the solution forms a network on the time scale of interest, and the rest of the molecules are allowed to diffuse within the pores of this network, it is clear that for the freely diffusing polymers with a large radius of gyration, α can be very large.

In addition, Slater and Wu[43] showed that when polymers are allowed to diffuse in a medium created by random removal of obstacles, interesting observations can be made. One of their results was that the molar mass scaling exponent was changed from 1, passing through a maximum of 2.4, as the matrix became more homogeneous. When unperturbed reptation became the dominant mechanism (the matrix became homogeneous), the scaling exponent was 2. In addition, they investigated the diffusion coefficient as a function of concentration. They arrived at the interesting result that the diffusion coefficient is not necessarily a strictly decaying function with concentration. They showed that as the solution became more and more concentrated, the diffusion coefficient decreased until a certain concentration of obstacles was reached, at which point it started to increase. Slater and Wu interpreted this as a change in diffusion mechanism, as did the authors in ref 26. The effect is thought to be a response to "entropic properties of flexible polymers in random environments, and the nature of the randomness in this environment".[26] This might explain the finding that the diffusion coefficient levels off with

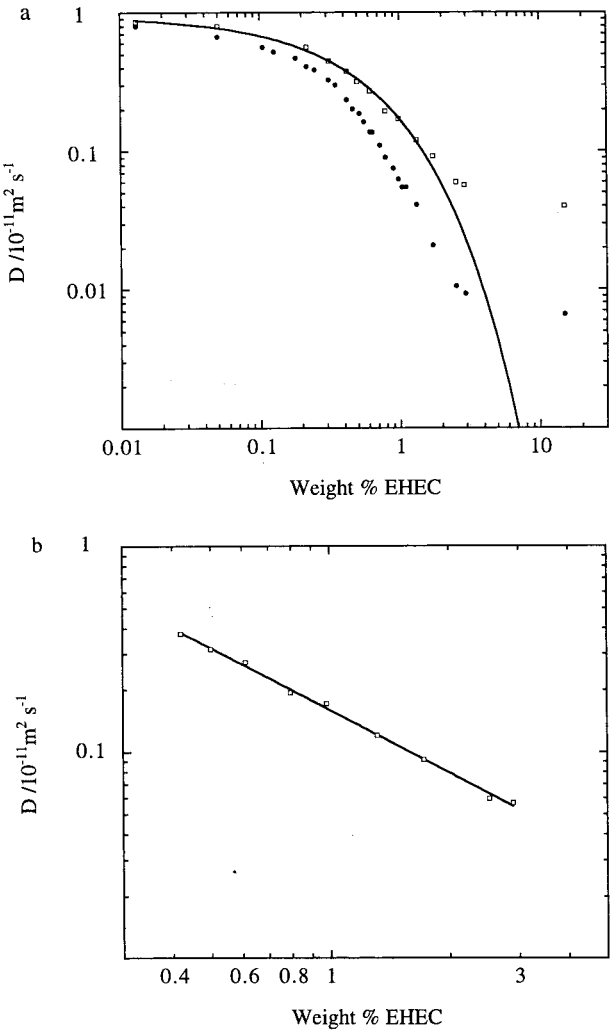

Figure 6. (a) Concentration dependence of the evaluated diffusion coefficients plotted on a log−log scale. (●) shows D_{mean}, obtained from eq 10, while (□) represents D_m in the log-normal distribution according to eq 13. It is clear that there is a large difference in using eq 10 or eq 13. For the higher concentrations of polymer, the results from the two equations differ almost by a factor 10. (b) Data from concentrations where D_m displays a power law dependence.

increasing concentration (cf. Figure 6), as observed here and by others.[26,27]

Concentration Dependence of *D*. We now examine the results from the concentration dependence of the diffusion coefficient in more detail. Although the initial part of the curve in Figure 6 shows a gradual change in D_m, it is clear that at higher concentrations the curve follows a power law dependence, as shown in the insert in Figure 6b. The reason for the continuous change in D_m is normally attributed to the concentration dependence of the monomer friction coefficient and the continuous change from Rouse to reptation dynamics.

Considering part b in Figure 6, it is clear that the data are more or less straight in the concentration region from 0.4 to 3 wt % (in the double logarithmic presentation). According to scaling theory, the diffusion coefficient scales as[50]

$$D \propto M^{-\alpha} c^{-y} \tag{15}$$

Here

$$y = \frac{\alpha - v}{3v - 1} \tag{16}$$

where α has its usual meaning. v is the molar mass scaling exponent of the diffusion coefficient for concentrations below c^*, the value of which is between 0.5 and 0.6 depending on the quality of the solvent. Here we note that the scaling exponent, y, in the case of unperturbed reptation dynamics is 1.75 in a good solvent. For trace amounts of poly(ethylene oxide) (PEO) diffusing in a 1% EHEC matrix, we observed $\alpha = 1$ (to be published). Since $y = 0.99$ for EHEC (see Figure 6), the obtained value of v is 0.5 in the linear concentration regime. This would indicate that water is a θ solvent for EHEC for concentrations ranging between 0.4 and 3%. However, one should bear in mind that this result is obtained from the molar mass scaling of a probe polymer, which is known not to interact strongly with EHEC, diffusing in a EHEC matrix.

Phillies challenges[20−23] the idea of a continuous crossover from Rouse to reptation dynamics. He bases his somewhat phenomenological theory on diffusion data from globular proteins in solution. Such data show a similar type of diffusion behavior, with respect to the concentration dependence of the diffusion coefficient. He argues that in these protein solutions the diffusion mechanism cannot be dominated by the reptation dynamics, due to the spherical symmetry of the proteins. In Figure 6 we show the fit of the theory by Phillies,[20] according to eq 17, to the concentration dependence of EHEC

$$D = D_0 \exp(-ac^b) \tag{17}$$

where D_0 is the diffusion coefficient at infinite dilution, a is a scaling prefactor and b is a streching exponent. The values obtained are $D_0 = 9.4 \times 10^{-12}$, $a = 1.71$, and $b = 0.71$. One striking feature is that the fit is more or less perfect for low concentrations but deviates above a certain concentration. [In the case of EHEC100 we conclude that eq 13 cannot describe the echo decay for the whole concentration range. We have to turn to eq 14 for concentrations above 0.2%. This indicates the formation of a static network or the presence of very large aggregates. We are thus forced to introduce additional parameters in order to describe the echo decay data. Consequently, the concentration dependence of D_m would not include the polymers present in the network/aggregates.] This effect has been observed in a number of previous works and is reviewed in reference 25. The deviation is explained by Phillies by the "gradual transition between solution to meltlike behavior". The same kind of behavior is often seen when measuring the molar mass dependence of the diffusion coefficient. However, the molar masses and concentrations used are often much higher than in this work.

Comparing the diffusion of EHEC and EHEC100, we note that the curvature in the echo decay starts to be pronounced at lower polymer concentrations for EHEC100 than for EHEC. This is shown in Figure 7, where we compare the echo decays of equal concentrations of EHEC and EHEC100. The curvature increases continuously as the concentration increases. In fact, the echo decays indicate the introduction of an additional diffusion mechanism. This is manifested as an apparent offset in the echo decay data. We interpret this offset

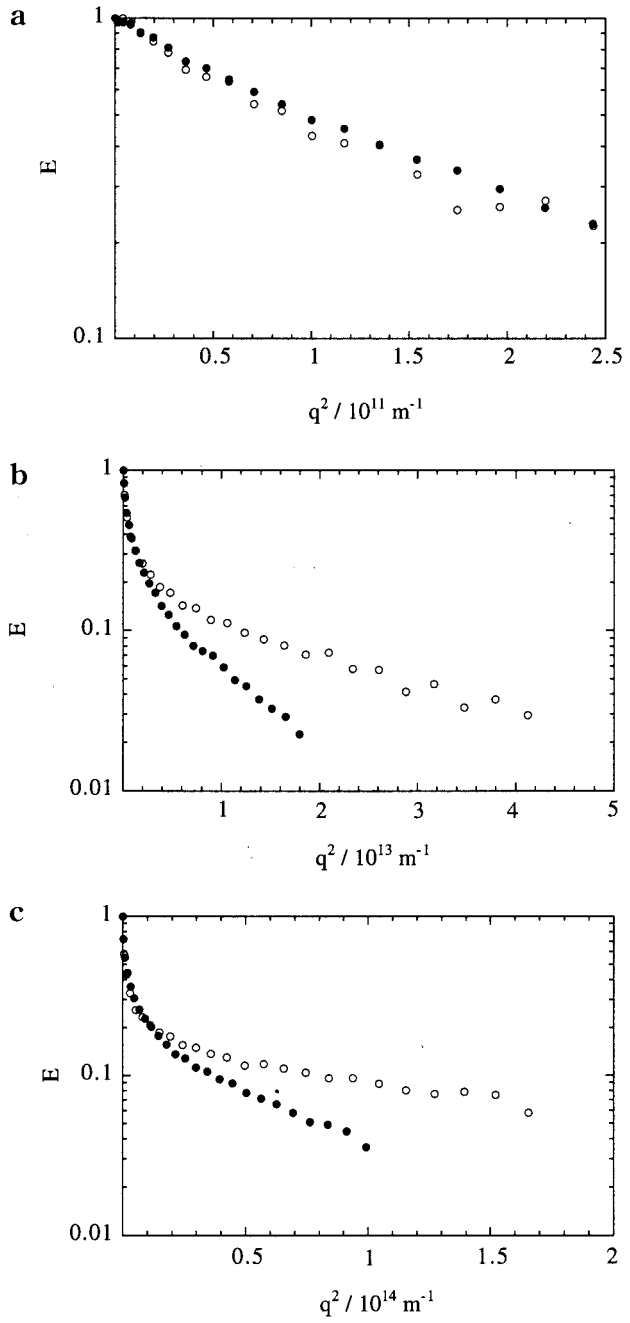

Figure 7. Comparison of the echo decays for similar concentrations of EHEC (●) and EHEC100 (○). The concentrations shown are (a) 0.013−0.013%, (b) 0.981−0.982%, and (c) 2.936−2.501% EHEC-EHEC100, respectively.

as the presence of a very slowly diffusing component. At this stage we also note that the same effect is seen for the EHEC polymer at higher concentrations. However, the contribution of the slow component is not as pronounced for EHEC as it is for EHEC100.

Coupling Theory of Ngai. In a recent paper by Ngai,[44] a theory is presented that connects the stretched exponent expression used by Phillies (cf. eqs 7 and 17) to the coupling theory by Ngai. We will not describe the coupling theory in detail, but a few words about the underlying ideas will be given. In polymer solutions, and in particular in systems that have a tendency to associate, one often finds that the time dependent concentration fluctuation, $\phi(t)$, may be described by a stretched exponential of the form

$$\phi(t) = \exp\left(-\left(\frac{t}{\tau}\right)^{1-n}\right) \tag{18}$$

here n is the coupling parameter and τ is the relaxation time. The value of n lies within the range $0 < n < 1$, and it is argued that n is a measure of the intermolecular interaction strength, which depends on the dynamical constraints experienced by the diffusing polymers. As a consequence, the dynamical/topological constraints are increased when the concentration is increased, and the factor $1 - n$ will decrease.[51]

From the stretched exponential form it is possible to calculate $n(c)$ from

$$n(c) = 1 - \frac{2}{3\nu + \dfrac{(3\nu - 1)\alpha(c^*)^u\left[\left(\dfrac{c}{c^*}\right)^u - 1\right]}{\ln\left(\dfrac{c}{c^*}\right)}} \tag{19}$$

where u, c^*, and $\alpha(c^*)$ follows from the fit of eq 20 to the D_m data in Figure 6.

$$D_m = D(c^*)\left(\frac{c}{c^*}\right)^{-y(c/c^*)} \tag{20}$$

Here

$$y\left(\frac{c}{c^*}\right) = \frac{\alpha(c^*)^u\left[\left(\dfrac{c}{c^*}\right)^u - 1\right]}{\ln\left(\dfrac{c}{c^*}\right)} \tag{21}$$

Using eqs 19−21 to fit the D_m data given in Figure 6, we obtain the values for the coupling parameter (n), as shown in Figure 8. The values of n have the same dependence on c/c^* as in the work presented by Ngai.[44] We notice that n takes on higher values already at low concentrations than the values of n presented for linear, nonassociating polymers by Ngai. In addition, we compare our results with the work of Abrahamsén et al.[26] They studied a monodisperse associative polymer (PEO with alkyl chain ends) and qualitatively observed the same effects in the echo decays as we find in the

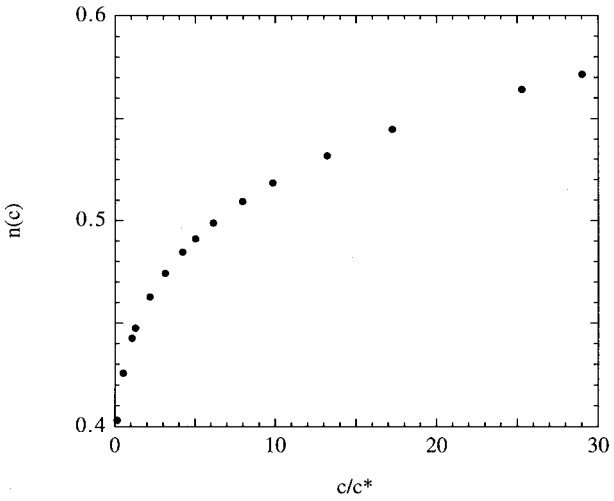

Figure 8. Coupling parameter (n) vs the normalized concentration c/c^* calculated by applying eqs 19−21 to the D_m data shown in Figure 6.

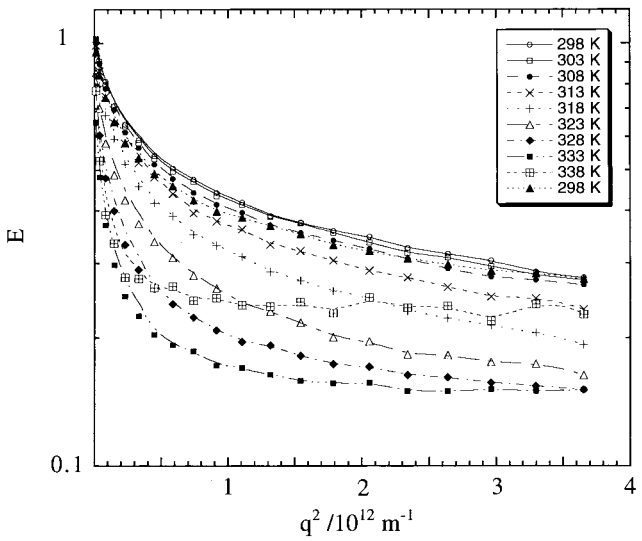

Figure 9. Echo decay for 1% EHEC100 for nine different temperatures. The data for 298 K were measured twice, before and after the various temperatures were measured, to make sure that the sample showed similar results before and after the change in temperature. The lines are guides for the eye.

EHEC system. Comparing the functional form of the coupling parameter as function of concentration, we conclude that their result is similar to the result presented in Figure 6. However, the strength of the interaction appears to be much stronger for EHEC than for the polymer studied in ref 26. Ngai also presents data for star polymers where the values for the coupling strength parameter resemble the values found in this work.

It should be pointed out that the coupling model when applied to self-diffusion data derived from PFG-NMR experiments does not take into account polydispersity effects. As far as the authors are aware, the coupling model takes into account polydispersity effects by assuming that the summation over the different-sized polymers can be included in a combined streching exponent (as extracted from dynamic light-scattering studies). However, to separate the coupling effect from the polydispersity effect is a difficult task. As a consequence, it has been argued that the value of n is underestimated for polydisperse systems.[44]

Temperature-Induced Aggregation. To shed some light on the mechanism of phase separation for EHEC100 in water and to learn more about the general diffusion mechanism, diffusion experiments were performed from 25 to 40 °C for a sample with 1% EHEC100 (recall that EHEC100 phase separates at 45 °C). In these experiments we have chosen to work with a constant range of q values and it is therefore informative to compare the echo decays for all temperatures. This is done in Figure 9.

Comparing the echo decays for the concentration dependence of EHEC and EHEC100 with the echo decays for the temperature dependence of EHEC100, we can conclude that some interesting comparisons can be made. The temperature dependence of EHEC diffusion close to the phase separation temperature was not investigated. The phase separation temperature for EHEC is 75 °C, and as a consequence, effects of convective flow induced by the temperature gradients in the NMR tube could not be neglected. As the concentration is increased for both EHEC and EHEC100, the curvature in the echo decays increases, as is also

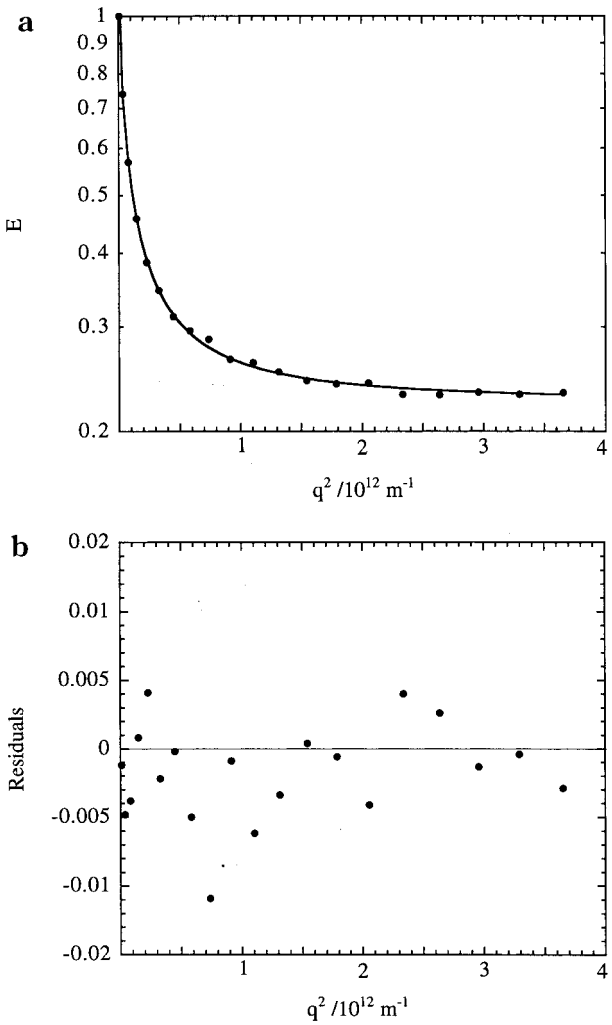

Figure 10. (a) Data set at 333 K for EHEC100. The solid line is the result of the fit of eq 14 to the data. Note that the residuals (b) are in all but one case smaller than 1% of the echo intensity, indicating a very good agreement between eq 14 and the echo decay data.

the case when temperature is increased for EHEC100. We note that the echo decay for EHEC100 can be separated into two main parts, as indicated by eq 14. With eq 14, D_s is locked to a value extracted from a single-exponential fit to the data that are linear on a log scale and f and D_m are fit parameters. The physical significance of eq 14 is the following. The first term on the right-hand side represents the formation of a static network that is shown as an offset (a very slowly diffusing species) in the echo decay. The second term represents the polymers that are aggregated and the diffusion coefficient of the aggregates are described with a log-normal distribution function. We note that the appearance of an offset in the echo decay data is probably present even at lower concentrations for EHEC100 and EHEC, but the fraction is so small that it cannot be extracted (the echo decay is not followed down to small enough values to see this diffusion mode). The results from the fit of eq 14 on the 333 K data are shown in Figure 10. In Figure 11 we show the values of f, σ, and D_m for the different temperatures. We observe a decrease in the log-normal distribution width, σ, when the temperature is increased. This is accompanied by an increase of D_m. We interpret this as an increase in the number of network contacts, thus leaving a smaller and smaller portion of the polymer

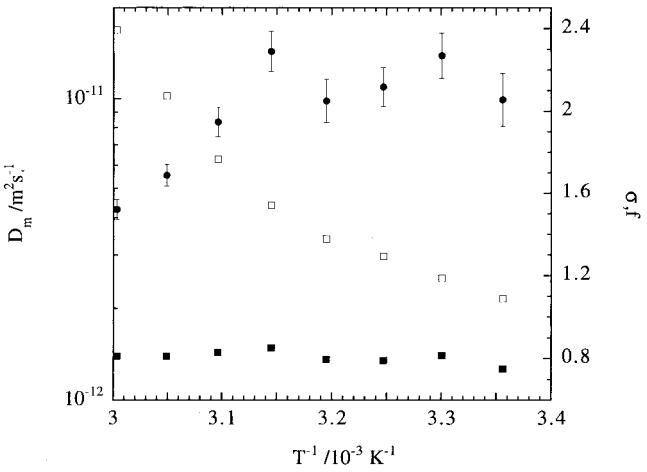

Figure 11. Parameters f, σ, and D_m as functions of the inverse temperature. (□) represents D_m, (■) shows the values of f, and (●) represents σ. For D_m and f, the errors are well represented by the size of the symbols. The y-axis on the left gives the D_m values and the right y-axis shows the values for f and σ.

left to diffuse freely in the solution as the temperature is increased. The freely diffusing polymers are necessarily polymers with a smaller molar mass than the polymers included in the network, since D_m increases when the temperature is increased. It thus appears that the temperature change causes a microscale fractionation of polymer molecules according to their size. We note in passing that since eq 14 is needed to describe the echo decay, it is difficult to apply the coupling theory to the temperature dependence of the coupling strength for EHEC100.

The results presented above indicate that the aggregation process affects the echo decay, in particular when increasing the temperature and/or the concentration. The aggregates form a network and create obstructing effects for polymers not included in the network, as discussed above. In addition, light-scattering data[45] and surface force measurements[46] have indicated the formation of some kind of "static" network as the concentration is increased.

There are several mechanisms that may cause aggregation in the polymer solutions presented here. One is connected with the solution properties of PEO/water mixtures. The properties of water[47] as a solvent for PEO have been investigated by a number of researchers and the mechanism is thought to be a change in the molecular conformation of PEO as a consequence of the change in the dipolar interactions between water and the PEO groups.[47,48] Water is a good solvent for PEO at low temperatures, but as the temperature is increased, the PEO changes structure and consequently the water solubility of the polymer changes. An example of this is seen in nonionic surfactant (of the C_mE_n type) systems, where the properties of the layer, separating hydrophobic and hydrophilic domains, are controlled by temperature. It is possible to reverse the curvature by a small change in the temperature.

A second mechanism for aggregation is the hydrophobic interaction. The strength of this interaction probably follows an Arrhenius type of behavior. We do not expect the hydrophobic effect alone, acting to drive the association of the hydrophobic tails substituted onto the backbone of the polymer, to play the central role for the change in the diffusion behavior when the temperature is increased. In addition, we note that the strength of the hydrophobic interactions decreases with an increase in temperature.

A third mechanism is the cellulose character of the polymer. Cellulose itself is not soluble in water (at normal pH) owing to the crystalline properties of the polymer. However, it is difficult to accept that an aggregation process, caused by the formation of crystalline parts, should be enhanced as the temperature is increased.

Relaxation. We now turn to the data from the relaxation measurements. An important factor that may complicate the interpretation of the PFG experiments is the ^{1}H NMR relaxation dependence on the polymer molar mass and concentration. Since the polymers differ in size, they will have different correlation times for tumbling. In effect, this means that both T_2 and T_1 may differ for different polymer sizes. For polymer melts, there is often a large dependence in both the T_2 and T_1 relaxation times on the molar mass. However, for solutions, T_2 does not differ between different molar masses, except for very low molar mass polymers. The same holds for the T_1 relaxation. This effect is normally attributed to the fact that $T_{1,2}$ is mostly governed by local segmental reorientation. In this work, experiments have been performed to try to verify this type of behavior. In general, the results from the two main EHEC ^{1}H NMR peaks at 0.8 and 3.7 ppm exhibit a typical biexponential decay with one relaxation time around 15−30 ms and the other at 0.3−0.5 s, with a fraction of 0.6−0.7 for the fastest relaxing species. The protons on the backbone itself most likely have a very fast T_2 relaxation due to the fact that the EHEC polymer is a stiff molecule. Therefore, these protons never contribute to the echo decay in a PFG NMR experiment. However, one can distinguish several different side chain protons that have been substituted onto the backbone, each of which can be considered to have different T_2 relaxation times. For a short side chain, the rotational motion of the chain is strongly influenced by the neighboring backbone, thus the relaxation will be faster. However, for a longer side chain, the effects of the backbone dynamics is decoupled from the side chain dynamics. This results in a longer relaxation time for the longer side chains. For samples with low concentrations of polymer, the relaxation measurements show a typical biexponential decay, independent of the peak chosen for the evaluation. For high concentrations, the situation is quite different, and a biexponential decay cannot be fitted to the relaxation data. However, the use of two stretched exponentials fits the echo decays well.

$$I = f_R I_0 \exp\left(-\frac{t}{T_2}\right)^{\beta^1} + (1 - f_R){I_0}^2 \exp\left(-\frac{t}{{T_2}^2}\right)^{\beta^2} \quad (22)$$

were f_R is the fraction of the fast relaxing species. In Figure 12, the echo decay in the "T_2" experiment for 15% EHEC is shown. The line is a fit to eq 22. The results from the fit are $T^1_{2,mean} = 0.4 \pm 0.15$ ms, $\beta_1 = 0.46 \pm 0.08$, $T^2_{2,mean} = 8.0 \pm 2.0$ ms, and $\beta_2 = 0.75 \pm 0.20$. $T^i_{2,mean}$ is calculated from eq 11. Note that in this case it is $\langle T_2 \rangle$ and not $\langle 1/T_2 \rangle$ that is measured.

One reason for the functional form of the echo decay in the relaxation experiment (and consequently the use of eq 22 in evaluating the data), could be the formation of a physical network (long-lived on the time scale of the measurement). The fast relaxing protons are the

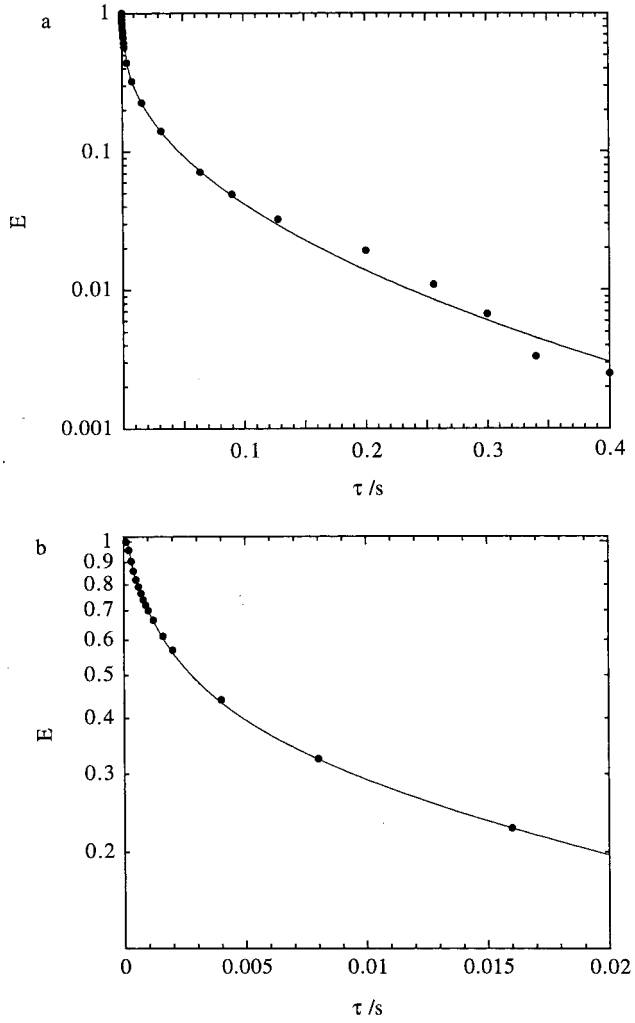

Figure 12. (a) Echo decay in the relaxation experiment for the 15% EHEC sample. The solid line is the fit of eq 22 to the data. Equation 22 was necessary for describing both the initial and final part of the decay. (b) Expansion of the same plot for small values of τ.

protons that are the connecting points between chains, and the reason for the spread in relaxation rates (as indicated by β_1) would be that protons situated at increasing distances from these connections, experience a decreasing restriction in motion. As the network mesh gets finer, i.e., when the polymer concentration increases, the fraction of connecting points increases. The slowly relaxing protons are the protons along the chain that are not tied up in the network. The fraction of these "free" protons would consequently decrease as the concentration is increased.

Conclusions

We have shown that the echo decays, in systems with a self-aggregating polymer, show large deviations from linear behavior when plotted in Stejskal−Tanner plots. The reason for this curvature is still not fully understood, but we conclude that by assuming a polydispersity in molar masses, a very strong scaling of the diffusion coefficient with the molar mass is needed to rationalize the data. In actual fact, the scaling exponent α takes values up to 4. Although computer simulations have shown that in some cases one can in fact enhance α by assuming a heterogeneous microstructure, we suggest that these large values of α indicate that an additional mechanism other than the polydispersity in polymer size, combined with a strong scaling dependence, is required to explain the data.

We focus on the use of the log-normal distribution of diffusion coefficient in evaluating the PFG NMR data. This approach yields values of D_m, which we use to extract information about Ngai's coupling parameter. We show that if these values are compared to previously presented values in systems that also show self-associating properties, we find that for EHEC there is a stronger dependence in the coupling strength as the concentration is increased. This effect is pronounced already at very low concentrations, indicating strong interactions.

We compare the echo decays of the polymer systems as the concentration is increased with the echo decay evolution by changing the temperature in a solution with fixed concentration of EHEC100. We conclude that the same trend with regard to the curvature in the echo decay applies for these two situations. This observation indicates that there is a strong interaction at room temperature, since it is known that at high enough temperatures the polymer will phase separate. During this process the polymers form large clusters and these finally cause phase separation. We show that the log-normal distribution width, σ, decreases when the temperature is increased, accompanied by an increase of D_m. It is argued that the rise in temperature enhances the number of network contacts, leaving a smaller portion of the polymer left to diffuse freely in the solution. Since σ decreases and D_m increases as the temperature is increased, the free polymers have a lower molar mass than the polymers included in the network. In addition, the distribution of these is narrower due to the microscale phase separation.

Finally, we note that the precise nature behind the curvature in the echo decay remains unknown.[55] To elucidate the precise mechanism behind this phenomenon, additional experiments are required. In particular, systems with a static network need to be thoroughly investigated. By chemically binding the polymers to each other and by letting different kinds of polymers diffuse in this matrix, we may hopefully extract more information about the true reason behind the echo curvature. Such experiments are underway.

Acknowledgment. Valuable discussions with Krister Thuresson are gratefully acknowledged. This work was financially supported by the Swedish Natural Science Research Council and by the Center for Amphifilic Polymers. The NMR spectrometer used was bought with a grant from the Swedish Council for Planning and Coordination of Research.

References and Notes

(1) Carlsson, A.; Karlström, G.; Lindman, B.; Stenberg, O. *Colloid Polym. Sci.* **1988**, *266*, 1031−1036.
(2) Carlsson, A.; Lindman, B.; Nilsson, P.-G.; Karlsson, G. *Polymer* **1985**, *27*, 431−436.
(3) Holmberg, C.; Nilsson, S.; Singh, S. K.; Sundelöf, L. O. *J. Phys. Chem.* **1992**, *96*, 871−876.
(4) Lindell, K. An Investigation of Thermogelling Aqueous Systems of Ethyl(Hydroxyethyl)Cellulose and Ionic Surfactants. Ph.D. Thesis, University of Lund, Sweden, 1996.
(5) Nilsson, S.; Holmberg, C.; Sundelöf, L.-O. *Colloid Polym. Sci.* **1994**, *272*, 338−347.
(6) Nilsson, S.; Holmberg, C.; Sundelöf, L.-O. *Colloid Polym. Sci.* **1995**, *273*, 83−95.
(7) Nilsson, S. *Macromolecules* **1995**, *28*, 7837, 7844.

(8) Nyström, B.; Walderhaug, H.; Hansen, F. K. *J. Phys. Chem.* **1993**, *97*, 7743−7752.
(9) Thuresson, K.; Söderman, O.; Hansson, P.; Wang, G. *J. Phys. Chem.* **1995**, *100*, 4909−4918.
(10) Thuresson, K.; Nilsson, S.; Lindman, B. *Langmuir* **1996**, *12*, 530−537.
(11) Thuresson, K. Solution properties of a hydrophobically modified polymer. Ph.D. Thesis, University of Lund, Sweden, 1996.
(12) Walderhaug, H.; Nyström, B.; Hansen, F. K.; Lindman, B. *J. Phys. Chem.* **1995**, *99*, 4672−4678.
(13) Zana, R.; Binana-Limbelé, W.; Kamenka, N.; Lindman, B. *J. Phys. Chem.* **1992**, *96*, 5461−5465.
(14) Callaghan, P. T.; Pinder, D. N. *Macromolecules* **1983**, *16*, 968−973.
(15) Callaghan, P. T.; Pinder, D. N. *Macromolecules* **1985**, *18*, 373−379.
(16) Fleischer, G. *Polymer* **1985**, *26*, 1677−1682.
(17) von Meerwall, E. D. *J. Magn. Reson.* **1982**, *50*, 409−416.
(18) von Meerwall, E. D. *J. Magn. Reson.* **1985**, *62*, 417−427.
(19) Callaghan, P. T. *Principles of Nuclear Magnetic Resonance Microscopy*; Oxford University Press: Oxford, U.K., 1991.
(20) Phillies, G. D. J. *Macromolecules* **1986**, *19*, 2367−2376.
(21) Phillies, G. D. J. *Macromolecules* **1987**, *20*, 558−564.
(22) Phillies, G. D. J.; Peczak, P. *Macromolecules* **1988**, *21*, 214−220.
(23) Phillies, G. D. J. *Macromolecules* **1988**, *21*, 3101−3106.
(24) Phillies, G. D. J. *J. Non-Cryst. Solids* **1991**, *131−133*, 612−619.
(25) Phillies, G. D. J. *J. Phys. Chem.* **1992**, *96*, 10061−10066.
(26) Abrahamsén-Alami, S.; Stilbs, P. *J. Phys. Chem.* **1994**, *98*, 6359−6367.
(27) Walderhaug, H.; Hansen, F. K. *J. Phys. Chem.* **1993**, *97*, 8336−8342.
(28) Walderhaug, H.; Nyström, B. *J. Phys. Chem. B* **1997**, *101*, 1524−1528.
(29) Callaghan, P. T. Personal communication.
(30) Morris, K. F.; Johnson, C. S., Jr. *J. Am. Chem. Soc.* **1992**, *114*, 3139−3141.
(31) Fujita, H. *Polymer Solutions*; Elsevier: Toyonaka, 1990.
(32) Richter, D.; Willner, L.; Zirkel, A.; Farago, B.; Fetters, L. J.; Huang, J. S. *Macromolecules* **1994**, *27*, 7−7446.
(33) Appel, M.; Fleischer, G. *Macromolecules* **1993**, *26*, 5520−5525.
(34) Callaghan, P.; Coy, A. *Phys. Rev. Lett.* **1992**, *68*, 3176−3179.
(35) Lodge, T. P.; Rotstein, N. A. *J. Non-Cryst. Solids* **1991**, *131−133*, 671−675.
(36) Käs, J.; Strey, H.; Sackmann, E. *Nature* **1994**, *368*, 226−229.
(37) Perkins, T. T.; Smith, D. E.; Chu, S. *Science* **1994**, *264*, 819−822.
(38) Smith, D. E.; Perkins, T. T.; Chu, S. *Phys. Rev. Lett.* **1995**, *75*, 4146−4149.
(39) Baumgärtner, A.; Muthukumar, M. *J. Chem. Phys.* **1987**, *87*, 3082−3088.
(40) Muthukumar, M.; Baumgärtner, A. *Macromolecules* **1989**, *22*, 1937−1941.
(41) Muthukumar, M.; Baumgärtner, A. *Macromolecules* **1989**, *22*, 1941−1946.
(42) Muthukumar, M. *J. Non-Cryst. Solids* **1991**, *131−133*, 654−666.
(43) Slater, G. W.; Wu, S. Y. *Phys. Rev. Lett.* **1995**, *75*, 164−167.
(44) Ngai, K. L. *Adv. Colloid Interface. Sci.* **1996**, *64*, 1−43.
(45) Thuresson, K.; Nyström, B.; Wang, G.; Lindman, B. *Langmuir* **1995**, *11*, 3730−3736.
(46) Freyssingeas, E. Personal communication.
(47) Andersson, M.; Karlström, G. *J. Phys. Chem.* **1985**, *89*, 4957−4962.
(48) Karlström, G.; Carlsson, A.; Lindman, B. *J. Phys. Chem.* **1990**, *94*, 5005−5015.
(49) Terentjev, E. M.; Callaghan, P. T.; Warner, M. *J. Chem. Phys.* **1994**, *102*, 4619−4624.
(50) Doi, M.; Edwards, S. F. *The theory of polymer dynamics*; Clarendon: Oxford, U.K., 1986.
(51) Ngai, K. L.; Phillies, G. D. J. *J. P. Chem. Phys.* **1996**, 105, 8385−8397.
(52) Buijtenhuijs, A.; Lecture presented at the Starch, Cellulose Derivatives Properties and Characterisation, Minisymposium, 1997, in Lund, Sweden.
(53) Nydén, M.; Stilbs, P. Unpublished data.
(54) Nyström, B.; Thuresson, K.; Lindman, B. *Langmuir*. **1995**, *11*, 1994−2002.
(55) As an indication of the complexity concerning the choice of evaluation procedure, we note that Terentjev et al.[49] have shown that PFG NMR experiments performed on particles trapped in a harmonic well also show a type of echo decay similar to that seen in this work. This effect is another possible contribution to the curvature in the echo decay as the concentration and/or temperature is increased, arising from the part of the polymer that is trapped between the hydrophobic “binding sites” or possibly from the polymer trapped inside the network. However, the q values needed to observe this type of mechanism are probably much higher than those investigated in this work.

MA971472+